Relaxation Processes in Harmonic Glasses?

G. Ruocco,[1] F. Sette,[2] R. Di Leonardo,[1] G. Monaco,[2] M. Sampoli,[3] T. Scopigno,[4] and G. Viliani[4]

[1]*INFM and Dipartimento di Fisica, Universitá di L'Aquila, I-67100, L'Aquila, Italy*
[2]*European Synchrotron Radiation Facility, B.P. 220, F-38043 Grenoble Cedex, France*
[3]*INFM and Dipartimento di Energetica, Universitá di Firenze, I-50139, Firenze, Italy*
[4]*INFM and Dipartimento di Fisica, Universitá di Trento, I-3805 Povo Trento, Italy*

(Received 6 December 1999)

A relaxation process, with the associated phenomenology of sound attenuation and sound velocity dispersion, is found in a simulated *harmonic* Lennard-Jones glass. We propose to identify this process with the so-called *microscopic* (or, instantaneous) relaxation process observed in real glasses and supercooled liquids. A model based on the memory function approach accounts for the observation and allows one to relate to each other (1) the characteristic time and strength of this process, (2) the low frequency limit of the dynamic structure factor of the glass, and (3) the high frequency sound attenuation coefficient, with its observed quadratic dependence on the momentum transfer.

PACS numbers: 63.50.+x, 61.43.Fs

In a recent paper Götze and Mayr [1] adapted the mode coupling theory (MCT) [2] to glassy phase. This theory, as shown numerically for a hard-spheres model, accounts for many of the features found in the dynamic structure factor, $S(Q,\omega)$, of glasses. Among these are (i) the existence of propagating excitations (sound waves), with an almost linear momentum transfer (Q) dependence of their excitation energy $\Omega(Q)$, up to Q values that are a significant fraction of Q_o, the maximum of the static structure factor $S(Q)$; (ii) the quadratic dependence on Q of the excitations broadening $\Gamma(Q)$, and therefore of sound attenuation; (iii) the temperature insensitivity of $\Gamma(Q)$; and (iv) the development in the $S(Q,\omega)$ at large Q ($Q/Q_o \approx 0.3$) of a secondary excitation band, at frequencies below the Brillouin peak. The theory also predicts two features not yet experimentally detected: (a) A positive dispersion of the sound velocity and (b) an intensity "gap" in the low frequency region of the $S(Q,\omega)$. In spite of the success of this approach, it is still of great interest to investigate the physical origin of these phenomena, and, in particular, whether they are related to the topological disorder and/or to the anharmonicity of the interatomic potential.

In this Letter we report a molecular dynamics (MD) simulation study of the Q dependence of the sound velocity in a model monatomic Lennard-Jones (LJ) glass in the *harmonic* approximation. We show that even in a *harmonic* glass, by increasing Q there is a positive dispersion of the sound velocity, thus proving one of the prediction of the MCT theory [1], and relating this phenomenon to the topological disorder. Since this dispersion is similar to that found in the presence of a relaxation process, we attempt to apply a generalized Langevin equation with an effective memory function approach to describe the density fluctuations dynamics. This formalism allows one to account for the ubiquitous Q^2 dependence of the high frequency sound absorption observed in many glasses by experiments [3] and by MD simulations [4,5]. These results suggest to identify this process with the one referred to as *microscopic* or *instantaneous* relaxation in *real* systems.

The investigated systems consist of $N = 2048$, 10 976, and 32 000 argon atoms interacting via a (6-12) Lennard-Jones potential ($\epsilon = 125.2$ K, $\sigma = 3.405$ A). A standard microcanonical classical MD simulation, performed at the constant density of $\rho = 42 \times 10^3$ mol/m^3 and at decreasing temperatures in the normal liquid phase, is followed by a fast quench ($\dot{T} \approx 10^{12}$ K/s) of the slightly supercooled liquid down to $\approx$5 K [6]. Starting from the glass configuration at $T = 5$ K, the atomic trajectories $\bar{r}_i(t)$ (here $i = 1, \ldots, N$ is the particle label) are followed and stored for subsequent analysis, and the "inherent" configuration $\{\bar{x}_i\}_{i=1,\ldots,N}$ [7] at $T = 0$ K is calculated by the steepest descent method. Two different procedures have been used to derive the $S(Q,\omega)$: (i) The trajectories calculated from MD in the glass are used to compute the corresponding time correlation function and (ii) the normal mode analysis (NMA) is applied to the inherent configuration. This last procedure works in the harmonic approximation, which is obtained by retaining only the quadratic term of the interaction potential. From the calculation of the dynamical matrix **D**, one computes the eigenvalues, ω_p ($p = 1, \ldots, 3N$ is the mode index) and the eigenvectors $[\bar{e}_p(i)]$. For large size samples (where a direct diagonalization of **D** is not feasible) the $S(Q,\omega)$ is obtained by the method of moments [8].

In the MD runs, the classical dynamics structure factor is calculated from the numerical time-Fourier transform of the intermediate scattering function $F(Q,t)$, defined as

$$F(Q,t) = 1/N\langle \Sigma_{ij} \exp[i\bar{Q} \cdot \bar{r}_i(t)] \exp[-i\bar{Q} \cdot \bar{r}_j(0)] \rangle . \quad (1)$$

In the harmonic framework and in the classical limit, the one excitation approximation of the dynamic structure factor $S^{(1)}(Q,\omega)$ is obtained by the normal mode expansion of the atomic displacements:

 0031-9007/00/84(25)/5788(4)$15.00

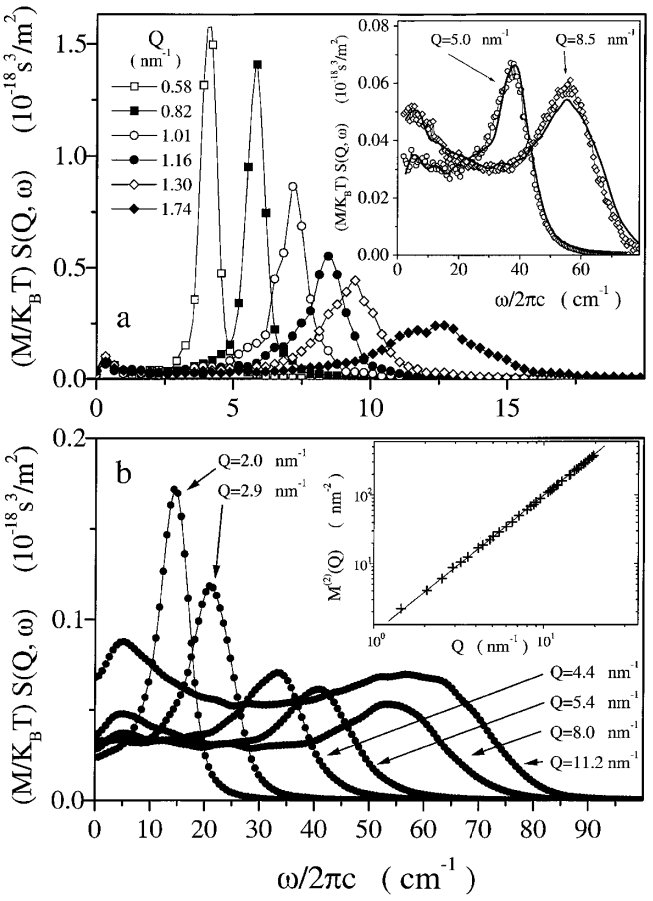

FIG. 1. The quantity $(M/K_BT)S(Q,\omega)$ is reported in absolute value at the indicated Q values for (a) the very low Q region ($N = 32\,000$, MD calculation) and (b) the intermediate Q region ($N = 2048$, NMA calculation). The inset of (a) shows the comparison ($N = 2048$) of the MD $S(Q,\omega)$ (full line) and the NMA $S^{(1)}(Q,\omega)$ ($\circ$). The inset of (b) shows the Q dependence of $M^{(2)}$, the second moment of $(M/K_BT)S(Q,\omega)$ (+), and its theoretical prediction $M^{(2)}_{\rm th} = Q^2$ (full line).

$$\bar{r}_i(t) = \bar{x}_i + \sqrt{K_BT/M}\,\Sigma_p \bar{e}_p(i)A_p(t)/\sqrt{\omega_p}\,. \quad (2)$$

$A_p(t)$ is the amplitude of the pth normal mode and is characterized by $\langle|A_p(t)|^2\rangle = 1$. This gives

$$S^{(1)}(Q,\omega) = (K_BTQ^2/M\omega^2)\Sigma_p E_p(Q)\delta(\omega - \omega_p), \quad (3)$$

where we have introduced the spatial power spectrum of the longitudinal component of the eigenvectors, $E_p(Q)$:

$$E_p(Q) = |\Sigma_i[\hat{Q}\cdot\bar{e}_p(i)]\exp(i\bar{Q}\cdot\bar{x}_i)|^2. \quad (4)$$

Here, $\hat{Q} = \bar{Q}/|Q|$ and the Debye-Waller factor has been neglected. Differently from the second [$\int \omega^2 S(Q,\omega)\,d\omega = \int \omega^2 S^{(1)}(Q,\omega)\,d\omega = K_BTQ^2/M$] and higher moments sum rules, the zeroth moment sum rule for $S(Q,\omega)$, $\int S(Q,\omega)\,d\omega = S(Q)$ does not hold for $S^{(1)}(Q,\omega)$, as in this function the elastic intensity is missing. Rather, it is useful to define the "inelastic" contribution to $S(Q)$: $S_i(Q) = \int S^{(1)}(Q,\omega)\,d\omega$.

Selected examples of the $S(Q,\omega)$ calculated for different size systems and with different methods are reported in Fig. 1. As there is a trivial dependence of the $S^{(1)}(Q,\omega)$ on T, here we report this quantity multiplied by the factor (M/K_BT). Figure 1a shows the $S(Q,\omega)$ in the low Q range, as calculated from the MD runs for the $N = 32\,000$ particles system, while Fig. 1b shows the intermediate Q range, in the case of the harmonic approximation for the $N = 2048$ system. As a check of consistency, the inset in Fig. 1b shows the Q dependence of the second moment of $(M/K_BT)S(Q,\omega)$ (+) which, according to the sum rule, should be Q^2 (full line). The inset of Fig. 1a shows, at two Q values, the comparison of the $S(Q,\omega)$ ($N = 2048$) calculated either from the MD runs (full line) or in the harmonic approximation ($\circ$). The $S(Q,\omega)$, as derived with the two different methods, are equivalent in the whole considered Q range. This indicates that the Newtonian dynamics at $T = 5$ K is truly harmonic and that the results obtained by MD at this T and NMA can be interchanged among each other.

The general features of the $S(Q,\omega)$ reported in Fig. 1 are: (i) a Brillouin peak, dispersing and becoming broader with increasing Q, dominates the spectrum up to $Q \approx 10$ nm^{-1} ($Q/Q_o \approx 0.45$). (ii) At larger Q values, a second peak below the Brillouin one starts to dominate the data. This secondary peak has been already detected in many systems: (1) in liquid water, both experimentally [9] and by MD [10], where it was interpreted as a signature of the transverse dynamics; (2) in vitreous silica, by MD, where it was interpreted either in terms of a transverse dynamics [5] or as an evidence of the boson peak [11]; and (3) in a hard sphere glass, where it was theoretically predicted [1]. In this respect, it is worth emphasizing the striking similarity between the $S(Q,\omega)$ reported here and those in Fig. 5 of Ref. [1]. Finally, (iii), the $S(Q,\omega)$ up to $Q \approx 5$ nm^{-1} shows a nearly constant and Q-independent intensity below the Brillouin peak frequency. This plateau, whose value is $\lim_{\omega\to 0}(M/K_BT)S(Q,\omega) = A_0 \approx 0.03 \times 10^{-18}$ s^3/m^2, can be identified with the plateau observed in the constant ω cuts of the $S(Q,\omega)$ at Q larger than the Brillouin peak in simulated [12], calculated (Fig 18 of Ref. [1]), and measured [13] systems.

Figure 2 shows the position of the maxima [$\Omega_c(Q)$] of the current spectra $C_L(Q,\omega)$ [$= \omega^2/Q^2 S(Q,\omega)$] as a function of Q in the investigated Q range. The inset in Fig. 2 shows the peak position $\Omega(Q)$ and the broadening $\Gamma(Q)$ of the $S(Q,\omega)$ in the low Q region, as measured directly from the spectra in Fig. 1a. The Q dependence of these parameters agrees with the behavior observed in all the glasses investigated so far [3]: a linear (square) dependence of $\Omega(Q)$ [$\Gamma(Q)$]. The behavior of $\Omega_c(Q)$ closely resembles that of the acoustic phonon branches in crystals, i.e., the almost linear behavior in the small Q region, a maximum around $Q_o/2$, and a minimum around Q_o. Most importantly one can clearly detect a positive dispersion of the sound velocity, as highlighted by the dashed line in Fig. 2. This dispersion is better seen in Fig. 3, where the apparent sound velocity, $v(Q) = \Omega_c(Q)/Q$, is reported [14]. The quantity $v(Q)$ (full dots) undergoes a transition from the "low frequency" [15] sound velocity $v_o(Q)$

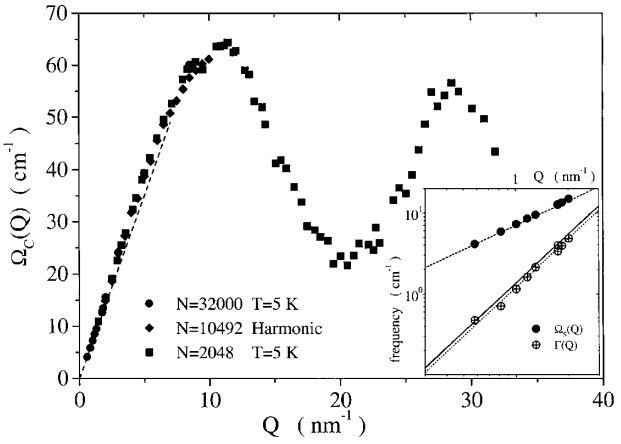

FIG. 2. Frequency position of the maxima of the longitudinal current spectra $[\Omega_M(Q)]$ for different indicated size samples. The inset shows in log-log scale the maxima $[\Omega(Q)]$ and the broadening $[\Gamma(Q)]$ of the Brillouin peaks in the low Q region. The full line is the prediction according to Eq. (11) and the dashed line is the best fit to the data.

towards the infinite frequency sound velocity $v_\infty(Q)$. Here $v_o(Q)$ is calculated as $v_o(Q) = \sqrt{K_B T/MS_i(Q)}$ (dashed line), and $v_\infty(Q)$ is calculated either as the fourth moment of the calculated $S(Q,\omega)$ (open points) or from the expression of the fourth moment in terms of both the pair correlation function and the interaction potential (full line) [16]. The velocity dispersion is observed up to $Q \approx 5$ nm^{-1}, i.e., $\Omega_c \approx 35$ cm^{-1}, and an opposite dispersion is observed in the region approaching Q_o. These observations recall a typical relaxation scenario. When a relaxation process with characteristic time τ is active in the system, the transition from v_o to v_∞ takes place when the condition $\omega\tau = 1$ is fulfilled. In the present case, considering that the first transition is at $Q \approx 2$ nm^{-1}, where $\Omega_c \approx 15$ cm^{-1}, the value of τ results to be around 0.3 ps. The second and third transitions between v_o and v_∞ are observed just below and above Q_o as a consequence of

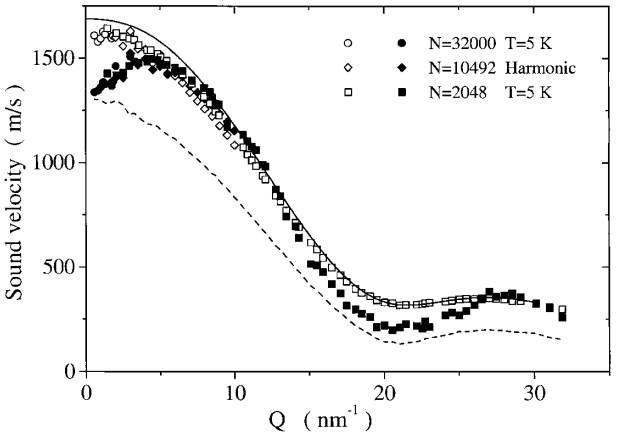

FIG. 3. Sound velocity in glassy LJ Argon: apparent sound velocity (v, full symbols), zero frequency sound velocity (v_o, dashed line), and infinite frequency sound velocity (v_∞, full line and open symbols).

the slowing down of the dynamics (de Gennes narrowing) around Q_o. Consequently the whole behavior of $v(Q)$, as reported in Fig. 3, can be qualitatively understood in terms of a relaxation process with a characteristic time of $\tau \approx 0.3$ ps.

The identification of such a *relaxation process* in a *harmonic system* suggests the use of formalism that describes the density correlators $\phi(Q,t) = F(Q,t)/S(Q)$ through its generalized Langevin equation [16]:

$$\ddot{\phi}(Q,t) + \omega_o^2\phi(Q,t) + \int_o^t m(Q,t-t') \times \dot{\phi}(Q,t')\,dt = 0, \quad (5)$$

where $\omega_o^2 = K_B T Q^2/MS(Q)$ and $m(Q,t)$ is the "memory function." This equation has been rigorously derived for ergodic systems, but, as recently shown in the framework of the MCT [1], it can still be applied in the nonergodic glassy phase making the following substitutions: $\phi(Q,t) \to \phi'(Q,t) = [\phi(Q,t) - f_Q]/(1-f_Q)$, $\omega_o^2(Q) \to \omega_{o\mu}^2 \equiv \omega_{\infty\alpha}^2 = K_B T Q^2/MS_i(Q)$, and $m(Q,t) \to m_\mu(Q,t) = m(Q,t) - \omega_o^2 f_Q/(1-f_Q)$. Therefore, the "vibrational" dynamics of interest is now described by the correlators $\phi'(Q,t)$, which is obtained subtracting from $\phi(Q,t)$ the long time plateau level, whose value is the nonergodicity parameter f_Q. It is worth noting that the subtraction of the constant term $S(Q)f_Q$ from $F(Q,t)$ is equivalent to neglecting the elastic contribution in the $S(Q,\omega)$, and that $F'(Q,t) = S_i(Q)\phi'(Q,t)$ is the Fourier transform of the $S^{(1)}(Q,\omega)$ as defined in Eq. (3). The whole dynamic behavior of $\phi'(Q,t)$ is now contained in the *microscopic* contribution to the memory function $m_\mu(Q,t)$. In a harmonic system, $m_\mu(Q,t)$ can be calculated from the eigenvalues and eigenvectors of the system. Indeed, the Laplace transform (hat) of Eq. (5), after the previously indicated substitutions and a straightforward algebra, gives

$$\hat{m}_\mu(Q,s) = \{\hat{\phi}'(Q,s)[s^2 + \omega_{o\mu}^2] - s\} \times [1 - s\hat{\phi}'(Q,s)]^{-1}. \quad (6)$$

Then, from an inverse Fourier and a subsequent Laplace transform of Eq. (3), it is easy to get an explicit expression for $\hat{\phi}'(Q,s)$ to be inserted in Eq. (6). This gives

$$\hat{m}_\mu(Q,s) = \left[\Sigma \frac{E_p(Q)}{\omega_p^2}\frac{s}{s^2+\omega_p^2}\right] \times \left[\Sigma \frac{E_p(Q)}{\omega_p^2}\Sigma \frac{E_p(Q)}{s^2+\omega_p^2}\right]^{-1} - s. \quad (7)$$

This equation provides an explicit expression of the memory function in terms of the system eigenstates. Considering that $m_\mu(Q,t)$ is mainly characterized by parameters as its initial value Δ_Q^2 and total area Γ_Q and therefore by a decaying time scale $\tau_Q \approx \Gamma_Q/\Delta_Q^2$ [17], one can show that $\hat{m}(Q, s\to\infty) = \Delta_Q^2/s$ and $\hat{m}(Q, s\to 0) = \Gamma_Q$ [16]. Inserting these limiting values into Eq. (7) one obtains

$$\Delta_Q^2 = [\Sigma_p E_p(Q)\omega_p^2] - [\Sigma_p E_p(Q)\omega_p^{-2}]^{-1}, \quad (8)$$

$$\Gamma_{\varrho} = \left[\Sigma_p \frac{E_p(Q)}{\omega_p^2}\right]^{-2} \lim_{s\to 0}\left[\Sigma_p \frac{E_p(Q)}{\omega_p^2}\frac{s}{s^2+\omega_p^2}\right]. \quad (9)$$

It is now easy to identify, through the explicit expression of the zeroth and fourth moments of Eq. (3), that $\Sigma_p E_p(Q)\omega_p^2 = v_\infty^2 Q^2$ and $[\Sigma_p E_p(Q)\omega_p^{-2}]^{-1} = v_o^2 Q^2$, confirming that $\Delta_{\varrho}^2 = (v_\infty^2 - v_o^2)Q^2$. The determination of Γ_{ϱ} which, being the area of the memory function, coincides with the Brillouin broadening in the $\omega\tau \ll 1$ limit is slightly more involved. Using the representation $\delta(x) = 1/\pi \lim_{s\to 0} s/(s^2 + x^2)$, in Eq. (3) one sees that

$$S^{(1)}(Q,\omega) = \frac{K_B T Q^2}{\pi M} \lim_{s\to 0}\Sigma_p \frac{E_p(Q)}{\omega_p^2}\frac{s}{s^2+(\omega-\omega_p)^2}, \quad (10)$$

and comparing Eqs. (10) and (9) one gets [18]

$$\Gamma_{\varrho} = v_o^4 Q^2 \frac{\pi M}{K_B T}\lim_{\omega\to 0} S(Q,\omega). \quad (11)$$

Similarly,

$$\tau_{\varrho} \approx \frac{v_o^4}{(v_\infty^2 - v_o^2)}\frac{\pi M}{K_B T}\lim_{\omega\to 0} S(Q,\omega). \quad (10)$$

Considering that $\lim_{\omega\to 0} S(Q,\omega)$ is Q independent (see Fig. 1), these expressions give account of the observation in the low Q region—where the Q dependence of v_o and v_∞ is negligible—that the Brillouin peak broadening is proportional to Q^2 and the τ is Q independent. Moreover, working in the harmonic limit, these equations indicate the temperature independence of Γ_{ϱ} and τ_{ϱ}. As a check of internal consistency, using the value of A_o previously reported, one finds $\tau \approx 0.6$ ps and $\Gamma_{\varrho}[\mathrm{cm}^{-1}] = 1.35 \times Q^2[\mathrm{nm}^{-1}]$. The value of τ_{ϱ} overestimates the one deduced from Fig. 3, and this is probably due to the rough expression of τ as $\Gamma_{\varrho}/\Delta_{\varrho}^2$. On the contrary, as shown in the inset in Fig. 2, Γ_{ϱ} from Eq. (11) is in excellent agreement with the one directly derived from the width of the $S(Q,\omega)$.

It is worth discussing the microscopic origin of the observed relaxation process. A relaxation process can be pictured as the macroscopic manifestation of microscopic phenomena associated with the existence of channels by which the energy stored in a given "mode" relaxes towards other degrees of freedom. The $S(Q^*,\omega)$, through the fluctuation-dissipation relation, reflects the time evolution of the energy initially stored ($t = t_o$) in a plane wave (PW) of wavelength $2\pi/Q^*$. As the PW is not an eigenstate of the disordered system, at $t > t_o$ there will be a transfer of amplitude from this PW towards other PWs of different Q values. This process is controlled by the difference between the considered PW and the normal modes of the topologically disordered glassy structure. This energy flow takes place on the time scale τ as derived from Eq. (12) and gives rise to the observed relaxation process phenomenology. Consequently, one can speculate that this process is the *instantaneous* or *microscopic* process empirically introduced to explain the $S(Q,\omega)$ measured in real glasses and liquids by Brillouin light and x-ray scattering [19,20].

We thank W. Götze for helpful discussions and critical readings of the manuscript.

[1] W. Götze and M. R. Mayr, Phys. Rev. E **61**, 587 (2000).

[2] W. Götze, J. Phys. Condens. Matter **11**, A1 (1999).

[3] F. Sette, M. Krisch, C. Masciovecchio, G. Ruocco, and G. Monaco, Science **280**, 1550 (1998), and references therein.

[4] S. N. Taraskin and S. R. Elliott, Phys. Rev. B **56**, 8605 (1997); Europhys. Lett. B **39**, 37 (1997); M. C. C. Ribeiro, M. Wilson, and P. A. Madden, J. Chem. Phys. **108**, 9027 (1998); J. L. Feldman, P. B. Allen, and S. R. Bickham, Phys. Rev. B **59**, 3551 (1999).

[5] R. Dell'Anna, G. Ruocco, M. Sampoli, and G. Viliani, Phys. Rev. Lett. **80**, 1236 (1998).

[6] V. Mazzacurati, G. Ruocco, and M. Sampoli, Europhys. Lett. **34**, 681 (1996).

[7] F. H. Stillinger and T. A. Weber, Phys. Rev. A **28**, 2408 (1983).

[8] C. Benoit, E. Royer, and G. Poussigue, J. Phys. Condens. Matter **4**, 3125 (1992); G. Viliani, R. Dell'Anna, O. Pilla, M. Montagna, G. Ruocco, G. Signorelli, and V. Mazzacurati, Phys. Rev. B **52**, 3346 (1995).

[9] F. Sette, G. Ruocco, M. Krisch, C. Masciovecchio, R. Verbeni, and U. Bergmann, Phys. Rev. Lett. **77**, 83 (1996); G. Ruocco and F. Sette, J. Phys. Condens. Matter. **11**, R259 (1999).

[10] M. Sampoli, G. Ruocco, and F. Sette, Phys. Rev. Lett. **79**, 1678 (1997).

[11] J. Horbach, W. Kob, and K. Binder, cond-mat/9901162.

[12] M. Sampoli, P. Benassi, R. Dell'Anna, V. Mazzacurati, and G. Ruocco, Philos. Mag. **77**, 473 (1998).

[13] F. Sette, G. Ruocco, A. Cunsolo, C. Masciovecchio, G. Monaco, and R. Verbeni, Phys. Rev. Lett. **84**, 4136 (2000).

[14] It is worth noting that in Ref. [1] the bend-up of the excitation dispersion relation (positive dispersion of the sound velocity) is accompanied by a slight bend-down occurring at smaller Q values. This phenomenon is not observed in our data as the positive dispersion of the sound velocity in LJ glasses takes place at Q values much smaller than in the case of hard-sphere systems.

[15] "Low frequency" means here the relaxed side of the *microscopic* relaxation process, which in a glass coincides with the fully unrelaxed, high frequency, side of the frozen structural (α) process.

[16] U. Balucani and M. Zoppi, *Dynamics of the Liquid State* (Clarendon Press, Oxford, 1994).

[17] This "relaxation time" τ_{ϱ} can be interpreted as the time needed by a set of harmonic oscillators of different frequencies to dephase each others.

[18] Equation (11) can also be derived from the Fourier transform of Eq. (5), i.e., $S(Q,\omega) = S(Q)\tilde{\phi}(Q,\omega) = S(Q) \times \omega_{o\mu}^2(Q)/\pi\omega \mathrm{Im}[\omega^2 - \omega_{o\mu}^2(Q) - i\omega\tilde{m}(Q,\omega)]^{-1}$, performing the $\omega \to 0$ limit, and remembering that the area of the memory function is $\tilde{m}'(Q,\omega = 0)$.

[19] H. Z. Cummins, J. Phys. Condens. Matter **11**, A95 (1999), and references therein.

[20] G. Monaco *et al.*, Phys. Rev. E **60**, 5505 (1999).